American Journal of Physical Chemistry
2022; 11(4): 91-101
http://www.sciencepublishinggroup.com/j/ajpc
doi: 10.11648/j.ajpc.20221104.12
ISSN: 2327-2430 (Print); ISSN: 2327-2449 (Online)

Use of Carbonaceous Materials Derived from Co-products of *Lophira lanceolata* for Adsorption Tests of Congo Red Dye

Elie Sogbochi[1, 2, 3], Pierre Girods[2], Guevara Nonviho[1], Sebastien Fontana[3], Yann Rogaume[2], Dominique Codjo Koko Sohounhloue[1, *]

[1]Laboratory of Study and Research in Applied Chemistry, University of Abomey-Calavi, Cotonou, Benin

[2]Laboratory of Study and Research on Wood Materials, University of Lorraine, Epinal, France

[3]Jean Lamour Institute, Joint Research Unit 7198 National Scientific Research Centre, University of Lorraine, Nancy, France

Email address:

csohoun@gmail.com (Dominique Codjo Koko Sohounhloue)

[*]Corresponding author

To cite this article:

Elie Sogbochi, Pierre Girods, Guevara Nonviho, Sebastien Fontana, Yann Rogaume, Dominique Codjo Koko Sohounhloue. Use of Carbonaceous Materials Derived from Co-products of *Lophira lanceolata* for Adsorption Tests of Congo Red Dye. *American Journal of Physical Chemistry.* Vol. 11, No. 4, 2022, pp. 91-101. doi: 10.11648/j.ajpc.20221104.12

Received: September 7, 2022; **Accepted**: September 29, 2022; **Published**: October 24, 2022

Abstract: The present study aims to valorize the hulls of *Lophira lanceolata*, an agricultural by-product in Benin. This natural resource, which is abundant in tropical countries, including Benin, has so far been considered as a biodegradable waste and treated as such. However, it has adsorption properties that can be exploited by transforming it into activated carbon for various uses, including water purification. For this purpose, activated carbons have been developed from the said hulls chemically impregnated with phosphoric acid. The adsorption kinetics of red Congo on these activated carbons is governed by the pseudo-second order kinetic model. The adsorption isotherms of Congo red by the Langmuir model give adsorbed quantities varying between 1250 and 1666.67 $mg.g^{-1}$, but this model is not credible to explain the mechanism. The Freundlich model is the most credible to explain the Congo red adsorption phenomenon. It indicates the cooperative and multilayer adsorption of Congo red on activated carbons. The thermodynamic study of the Congo red adsorption process shows that it is exothermic, spontaneous, and the Congo red molecules fixed are ordered on the surface of the activated carbons. Thus, it should be noted that the adsorbents produced can be used for the removal of anionic dyes in aqueous solution and effective at low concentrations.

Keywords: *Lophira lanceolata*, Biomass, Activated Carbon, Red Congo, Adsorption

1. Introduction

Today, industrial, and domestic discharges loaded with synthetic dyes and chemicals are leading to increased degradation of water resources and the environment. Effluents discharged from paper, textile, plastic, printing industries, etc. contaminate water resources and cause high chemical oxygen demand, resulting in carcinogenic and mutagenic effects on plants, humans and aquatic life [1].

Among these, Congo red has many harmful effects on the environment such as eutrophication and endangers human life with diseases such as drowsiness, skin and eye irritation and respiratory problems [1]. In the colour index classification system, it is considered an anionic dye [2]. Furthermore, Congo red, also known as benzidinediazo-bis-1-naphthylamine-4-sulphonic acid, is a complex molecule and therefore difficult to remove. It is therefore necessary to eliminate it from effluents because of its harmful effects on humans and the environment [3].

Due to their good water solubility and mobility, these pollutants are likely to reach downstream drinking water and can pose a huge risk to people, even at low concentrations.

Today, the use of conventional and emerging adsorbent materials is an attractive method at the heart of technological

and environmental challenges. There are five main types of adsorbents: activated carbons, zeolites, aluminas, silica gels and activated clays [4–7]. To these can be added other emerging materials, such as MOFs, COFs, composite materials, etc [8, 9]. However, activated carbons remain the main adsorbents used. They are essentially carbonaceous materials with very high porosity and highly developed internal and external surfaces. They come from three sources: precursors of fossil origin, materials of vegetable origin and sometimes synthetic materials. Numerous studies have valorized lignocellulosic residues as activated carbons for the depollution of liquid and gaseous effluents [10]. It appears that wood residues, coconuts, banana peels, rice rejects, jengkol shells, etc. have a huge potential for pollutant adsorption. Biomass from the production of vegetable oils is rarely exploited, yet their valorization could contribute to curb the systematic felling of plant species and their impact on the environment.

The objective of the present article is to continue the work on the elaboration of activated carbons from *Lophira lanceolata* hulls by applying the latter for adsorption tests, in particular the removal of anionic dyes such as Congo red. Indeed, the effect of contact time and temperature on the adsorption capacity, the adsorption kinetics, the modelling of the isotherms and the explanation of the molecules of red Congo fixation mechanism are studied.

2. Materials and Methods

2.1. Materials

The hulls of *Lophira lanceolata* were collected in Toucountouna, a community located in the North-West of Benin. NaOH (Merck) was used to remove fat from the hulls. H_3PO_4 (Merck) was used as an activating agent. Hydrochloric acid (Merck) and distilled water to wash the activated carbons. Red Congo (Merck) was used as an adsorbate to test the adsorption performance of activated carbons.

2.2. Synthesis Activated Carbons of Lophira lanceolata Hulls

The activated carbons were produced according to the diagram in Figure 1. The hulls of *Lophira lanceolata* were crushed and sieved to a size below 5 mm. The resulting material was washed, rinsed, and dried in an oven at 103°C for 24 hours. It's then washed with enough molar soda solution and dried in an oven at 103°C for 24 hours. Standard scheme treatments were applied as follows: (1) The pretreated material was washed with tap water until its pH returned to that of the water used and then dried again in an oven at 103°C. (2) After 24 hours, they were impregnated with 50% diluted orthophosphoric acid in three different ratios ($m_{H_3PO_4}$ / $m_{Precursor}$): 1:1; 2:1; 3:1; 4:1 and the mixtures were dried at 103°C in an oven for 24 hours. (3) Then, they were carbonized in an oven at 500°C, with the heating rate of 10°C/min. (4) At the final temperature, after a stay of 2 hours, the coal was properly washed with a decimolar solution of hydrochloric acid and then with distilled water.

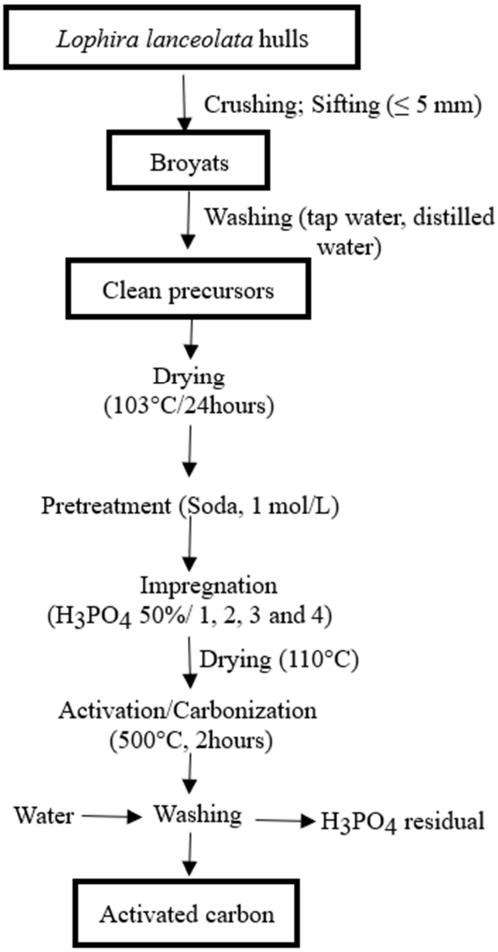

Figure 1. *The diagram of the elaboration of activated carbons from Lophira lanceolata hulls.*

2.3. Study of the Adsorption of Chemical Dyes on Adsorbent Materials

2.3.1. Effect of Contact Time

Adsorption was studied as a function of time to determine the amount of dye adsorbed at different time intervals and the equilibrium time. A mass m of activated carbon was suspended in a solution of volume V and initial concentration C_0. Samples were taken at predetermined time intervals and separated using a syringe equipped with filters (0,45µm). The analysis of the residual concentration of the adsorbates (Table 1) was performed by UV-Visible absorption spectrophotometry, where the dye solution absorbs lighter. The results obtained are plotted in the form of curves $q_t = f(t)$ and $R(\%) = f(t)$. The amount of adsorbed dye $q_t(mg/g)$ and the removal rate R (%) are calculated as follows [11–13]:

$$q_t = \frac{(C_0 - C) \times V}{m} \quad (1)$$

$$R(\%) = \frac{C_0 - C}{C_0} \times 100 \quad (2)$$

where C_0 and C are the initial adsorbates concentration (mg. L^{-1}) and at time t (min). V is the volume of solution (L) and m the dry weight of the added adsorbent (g).

Table 1. *Information on the dye that was the subject of this study [14, 15].*

Type	Red Congo
Gross formula	$C_{32}H_{22}N_6O_6S_2Na_2$
Semi-developed formula	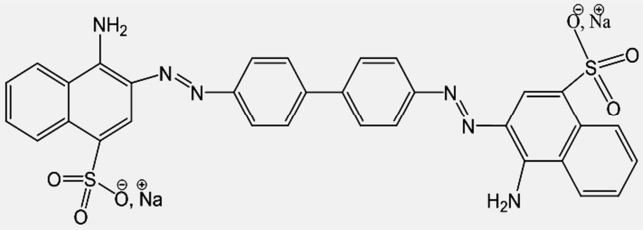
IUPAC name	Benzidinediazo-bis-1-naphthylamine-4-sulfonic acid
Wavelength (nm)	500
Molecular molar mass ($g.mol^{-1}$)	696,663 ± 0,04

2.3.2. Kinetic Study of the Adsorption of Chemical Dyes on Adsorbent Materials

The study of adsorption kinetics is important to be able to define the adsorption efficiency.

To study the kinetics and determine its parameters, the experimental data were analyzed using pseudo-first order, pseudo-second order, Elovich and intraparticle diffusion models.

1) Pseudo-First Order Kinetic

The pseudo-first order Lagergren velocity equation is expressed as the following differential equation [16]:

$$\frac{dq}{dt} = k_1(q_e - q_t) \quad (3)$$

With q_e is the adsorption capacity on activated carbon at equilibrium (mg/g), q_t the adsorption capacity on the activated carbon at the instant t (mg/g) and k_1 the kinetic constant of the adsorption reaction (min^{-1}).

The integration of equation 10 gives:

$$\ln(q_e - q_t) = \ln q_e - k_1 t \quad (4)$$

2) Pseudo-second order kinetic

The pseudo-second order model is given by the following differential equation [17]:

$$\frac{dqt}{dt} = k_2 (q_e - q_t)^2 \quad (5)$$

Where k_2 is the second order reaction rate constant of adsorption of on activated carbons ($g.mg^{-1}.min^{-1}$).

q_e the quantity adsorbed at equilibrium (mg/g), q_t the quantity adsorbed at time t (mg/g) and t the contact time (min).

After integration we obtain:

$$q_t = \frac{k_2 q_t}{1 + k_2 q_e t} \quad (6)$$

The linearization of the previous equation gives [18]:

$$\frac{t}{q_t} = \frac{1}{k_2 q_e^2} + \frac{t}{q_e} \quad (7)$$

We plot t/q_t = f(t) and get a straight line that gives k_2 and q_e.

3) Intraparticle diffusion

This model is based on molecular diffusion. Also known as the Weber and Morris model, it was developed to determine the type of diffusion mechanism involved in the adsorption phenomenon. The intraparticle diffusion constant ki is determined by this model represented by the equation 8 [19]:

$$q_t = k_i t^{1/2} + c \quad (8)$$

q_t: is the quantity adsorbed at time t (mg/g) and c: is the intersection of the straight line with the y-axis or the intercept at the origin.

4) Elovich kinetic model

This model is given by the differential equation (9):

$$\frac{dq_t}{dt} = \exp(-\beta q_t) \quad (9)$$

To simplify the Elovich equation it has been assumed that $\beta t \gg \alpha$ and that $q_0 = 0$ to $t_0 = 0$, so we obtain the linear form after the integration [20]:

$$q_t = \frac{1}{\beta}\ln(\alpha\beta) + \frac{1}{\beta}\ln(t) \quad (10)$$

α: initial adsorption rate (mg/g.min); $t_0 = 1/(\alpha.\beta)$ et β: constant related to the external surface and the activation energy of chemisorption ($g.mg^{-1}$).

2.3.3. Study and Modeling Adsorption Isotherms

1) Langmuir Isotherm

It corresponds to isotherms of type L and is given by the following equation [21]:

$$q_e = \frac{q_m k_L C_e}{1 + k_L C_e} \quad (11)$$

q_e is the amount adsorbed at equilibrium($\mathrm{mg.g^{-1}}$), C_e the solution concentration at equilibrium ($\mathrm{mg.L^{-1}}$), q_{max} : represents the maximum adsorption capacity of the solid phase loading ($\mathrm{mg.g^{-1}}$) and K_L: Langmuir Coefficient. It is an indicator of the affinity of the adsorbate for the adsorbent, the higher the coefficient, the stronger the affinity. The Langmuir isotherm assumes homogeneity of the adsorbent surface and is represented by the following equation [22]:

$$\frac{C_e}{q_e} = \frac{1}{q_m K_L} + \frac{C_e}{q_m} \quad (12)$$

The plot of $\frac{C_e}{q_e} = f(C_e)$ allows to determine the isothermal constants.

2) Freundlich Isotherm

This model establishes a relation between the quantity adsorbed and the quantity remaining in the liquid phase, its equation is based on an exponential distribution of the energies of the adsorption sites, it is expressed by the relation 13 [23]:

$$q_e = K_F C_e^{\frac{1}{n}} \quad (13)$$

The linear form is the equation 14 [16]:

$$\ln q_e = \ln K_F + \frac{1}{n}\ln C_e \quad (14)$$

Where q_e: quantity adsorbed per unit mass of the adsorbent (mg/g); Ce: residual concentration of the adsorbate at equilibrium ($\mathrm{mg.L^{-1}}$); K_F and n: Freundlich constants related to adsorption capacity and adsorption intensity, respectively.

3) Tempkin Isotherm

Tempkin's model explicitly considers the interactions between the adsorbed species and the adsorbent. It also predicts that the heat of adsorption of all molecules in the layer would decrease linearly with the blanket involved in this interaction. The linear shape of the model of Tempkin is expressed as follows [16]:

$$q_e = B\ln A + B\ln C_e \quad (15)$$

Where

$$B = \frac{RT}{b} \quad (16)$$

With A, the equilibrium binding constant of Tempkin ($\mathrm{L.mg^{-1}}$) corresponding to the maximum binding energy and B, the constant related to the heat of adsorption. T is the absolute temperature and R is the universal perfect gas constant.

2.3.4. Influence of Temperature on the Adsorption of Red Congo

The effect of temperature on adsorption is associated with several thermodynamic parameters. For this purpose, we introduced in several Erlenmeyers 100g of carbonaceous materials and 50mL of the solution of concentration equal to $\mathrm{100mg.L^{-1}}$. The whole was stirred at 100 rpm and the influence of temperature was studied with solutions at 20, 35 and 50°C.

We have used the following equations to calculate the thermodynamic parameters:

$$\Delta G° = \Delta H° - T\Delta S° \quad (17)$$

$$\ln(K_e) = \frac{\Delta S°}{R} - \frac{\Delta H°}{RT} \quad (18)$$

With $K_e = \frac{q_e}{C_e}$: Equilibrium constant, $\Delta H°$: Enthalpy variation ($\mathrm{kJ.mol^{-1}}$), $\Delta S°$: Entropy variation ($\mathrm{J.mol^{-1}.K^{-1}}$), T: Temperature (K), R: Constant of perfect gases (R= 8,314 $\mathrm{J.mol^{-1}.K^{-1}}$), q_e: quantity adsorbed at equilibrium ($\mathrm{mg.g^{-1}}$) and Ce: Concentration at equilibrium ($\mathrm{mg.L^{-1}}$).

2.3.5. Error Functions Used in the Selection of Appropriate Models

The coefficient of determination (R^2), the sum of square errors (SSE, %) and the average relative error (ARE, %) are used to compare the experimental data and the results predicted by each model. The higher the R^2 value, the smaller the mean relative error and the smaller the sum of squared errors, the better the fit. The sum or error squares (SSE, %) given by:

$$SSE\ (\%) = \sum_{i=1}^{N}(q_{e,exp} - q_{e,cal})_i^2 \quad (19)$$

The average relative error (ARE,%) given by [24, 25]:

$$ARE(\%) = \frac{100}{N}\sum_{i=1}^{N}\left|\frac{q_{e,exp}-q_{e,cal}}{q_{e,exp}}\right|_i \quad (20)$$

where N is the number of data points.

3. Results and Discussion

3.1. Influence of Contact Time on the Adsorption Capacity of Red Congo

The experimental results indicate a rapid increase in adsorption capacity during the first few minutes; this shows that the adsorption speed is high at the beginning of the reaction as illustrated in Figures 2 and 3. Activated carbons removed the Congo red molecules with a removal rate of about 50%.

The results show a rapid increase in the binding capacity of the molecules of the red Congo within the first 10 minutes of contact. Saturation is reached before 60 minutes of reaction. The maximum removal capacity obtained for all materials is less than 100 $\mathrm{mg.g^{-1}}$. The elimination of Congo red is difficult because of its complex structure and the fact that it is anionic.

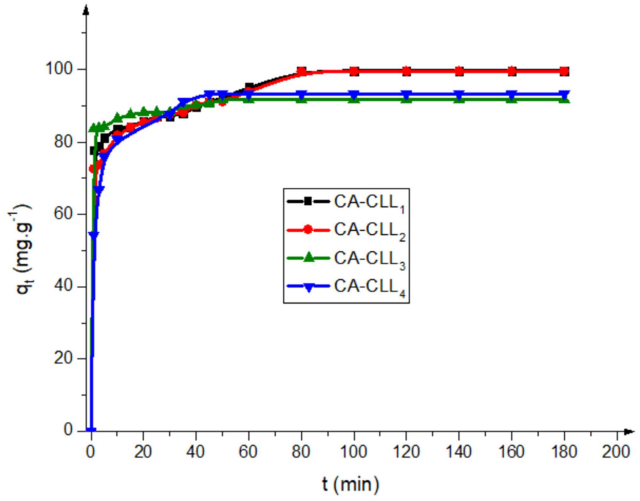

Figure 2. *Influence of contact time on the quantity of red Congo adsorbed onto the activated carbons.*

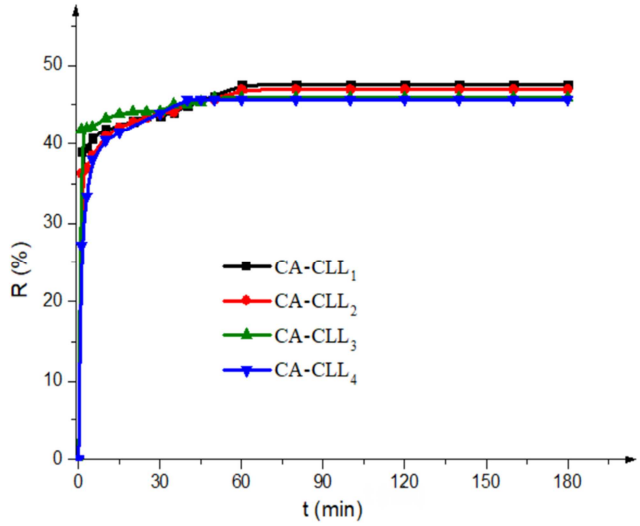

Figure 3. *Influence of contact time on the rate of red Congo adsorbed by the activated carbons.*

3.2. Study of the Adsorption Kinetics of Red Congo on Activated Carbons

The kinetic models were applied to the adsorption of Congo red on the activated carbons (Figures 4, 5, 6 and 7). The coefficients of determination of the pseudo-second order kinetic model are the highest, so it is the most appropriate to explain these adsorption processes (Table 2). In addition, this model has the closest calculated adsorbed quantities to the experimental one; its SES (%) and ARE (%) are the lowest (Table 2). This indicates that the adsorption is perfectly consistent with the pseudo-second order reaction and that the adsorption processes appears to be controlled by the chemisorption [21]. Several works in the literature have shown that the adsorption of Congo red is controlled by second order kinetics and is chemical [3, 21, 22].

The Elovich model assumes that the adsorption sites increase exponentially with adsorption. As can be deduced, the Elovich kinetic model appears to be insufficient to describe the adsorption of red Congo due to the low R^2 values, indicating that there are several mechanisms involved in the adsorption processes [25]. The intra particle diffusion model plotted should be linear if intra particle diffusion is involved in the adsorption process and when these curves pass through the origin of the benchmark. If the curves do not pass through the origin, this indicates some degree of boundary layer control and shows that intra particle diffusion is not the only rate-limiting step, but that other kinetic models could control the rate of adsorption. Figure 6 shows that the curves are multilinear over the entire selected time range, implying that more than one process affects adsorption and that the adsorption processes contains both surface adsorption and diffusion within the solid support. The adsorption of these molecules might not be controlled by diffusion due to the high presence of micropores and mesopores.

1) Pseudo-first-order kinetics

The plot of the linear form of this model by the formula (4):

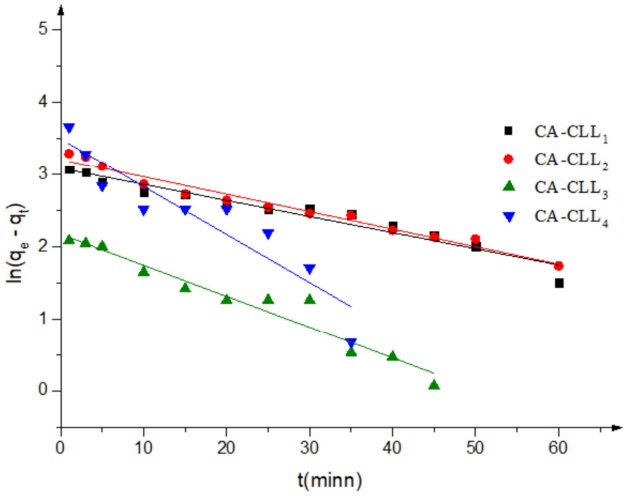

Figure 4. *Linearized forms of the pseudo-first order model of red Congo adsorption.*

2) Pseudo-second-order kinetics

The plot of the linear form of this model by the formula (7):

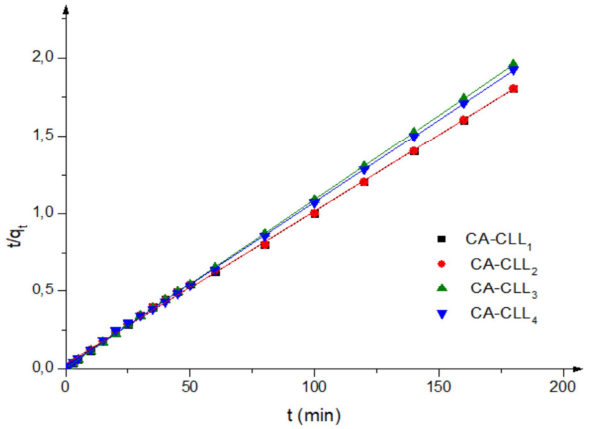

Figure 5. *Linearized pseudo-second order forms for red Congo adsorption.*

3) Intra particle diffusion

The intra particle diffusion model shown in Figure 6:

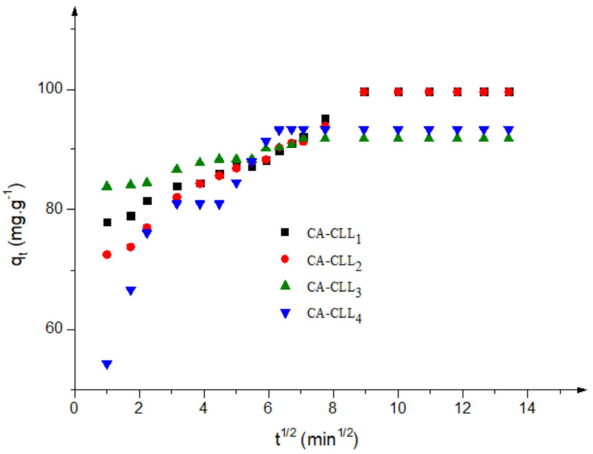

Figure 6. *Intraparticle diffusion model of red Congo adsorption.*

4) Kinetic model of Elovich

This model was illustrated in Figure 7:

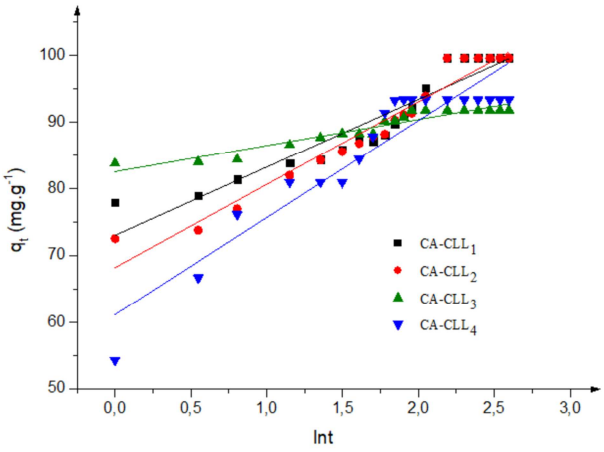

Figure 7. *Linearized forms of the Elovich model of red Congo adsorption.*

3.3. Isotherms of Adsorption of Red Congo onto Carbonaceous Materials

Table 2. *Kinetic parameters of adsorption models on activated carbons.*

		CA-CLL$_1$	**CA-CLL$_2$**	**CA-CLL$_3$**	**CA-CLL$_4$**
	C_0 (mg.L^{-1})	200	200	200	200
	$q_{e,exp}$(mg.g^{-1})	95,16	93,94	91,84	91,44
	$q_{e,cal}$ (mg.g^{-1})	21,93	24,85	8,81	33,05
	K_1 (min^{-1})	2,22.10^{-2}	2,42.10^{-2}	4,65.10^{-2}	6,63.10^{-2}
Pseudo-first-order	r_1^2	0,94159	0,96794	0,94066	0,85169
	SSE (%)	5362,84	4773.21	6894,15	3409,32
	ARE (%)	5,92	5,66	8,22	7,10
	$q_{e,cal}$ (mg.g^{-1})	100	95,24	92,59	92,60
	K_2 (g.min.mg^{-1})	5,30.10^{-3}	6,60.10^{-3}	1,72.10^{-2}	9,18.10^{-3}
Pseudo-second-order	r_2^2	0,9997	0,9999	1	0,9998
	SSE (%)	23,43	1,69	0,57	1,33
	ARE (%)	0,27	0,07	0,04	0,066
	α	13208,35	3030,17	5,22.10^{9}	981,35
Elovich model	β	9,81.10^{-2}	8,05.10^{-2}	0,25	6,88.10^{-2}
	r^2	0,89029	0,95254	0,91247	0,87876
	k_i	1,97	2,29	0,6859	0,8521
Intra particle diffusion	C	77,31	74,14	84,69	84,24
	r^2	0,9333	0,9098	0,7824	0,4007

Figure 8 present the adsorption isotherms of Congo red on activated carbons produced. It is important to emphasize that the initial concentrations of Congo red used during the studies of the isotherms are relatively high (50 and 1500 mg.L^{-1}) compared to other studies reported in the literature. The isotherms for the adsorption of Congo red on activated carbons have the form of an S-type isotherm (Figure 8). This is therefore an adsorption in which the interactions between the molecules and the molecules-adsorbent intervene. Consequently, the adsorption of Congo red could be multilayer and cooperative. However, the interactions are often opposite phenomena, because the interaction between the molecules could hinder their fixation on the surface of the solid support.

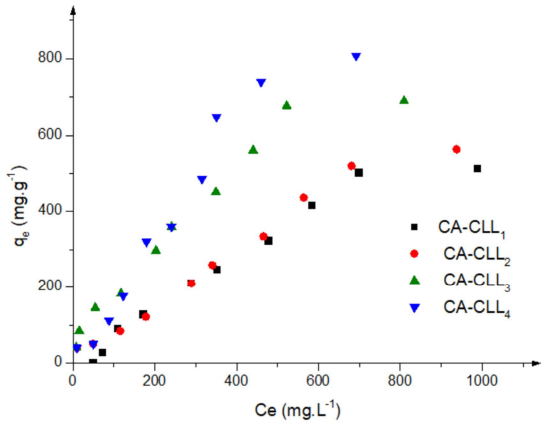

Figure 8. *Adsorption isotherms of red Congo on activated carbons.*

3.4. Modelling Isotherms of Red Congo Adsorption on Activated Carbons

The linear Langmuir, Freundlich and Tempkin models are shown on Figures 9, 10 and 11 and their calculated constants are given in Table 3. These results show that the Langmuir model is not the most suitable model to describe the experimental results from red Congo adsorption. The maximum adsorption capacities according to the Langmuir model are presented in Table 3, but it is not credible to explain this adsorption phenomenon because its correlation coefficient is very low. The maximum adsorption capacities according to the Langmuir model are presented in Table 3 with $q_{max} = 1250{,}00$; 1428,57 ; 1587,30 and 1666,67 $mg.g^{-1}$, but it is not suitable for explaining this adsorption phenomenon because its correlation coefficient is low. The Freundlich model ($R_F^2 > R_T^2 > R_L^2$) was found to be the most credible model to explain this reaction. Furthermore, the Freundlich model confirms the cooperative and multilayer adsorption of Congo red on activated carbons. This model, with its constant 1/n greater than 1, shows that the adsorption of Congo red on activated carbons encounters obstacles and is therefore not favourable.

Table 4 summarizes the adsorption capacity of red Congo of different activated carbons prepared from agricultural waste. The maximum adsorption capacities obtained in this study are very high compared to those in the literature presented. The very high initial concentration (up to 1,500 mg. L^{-1}) used in this study could be the basis for the high quantity of molecules observed at equilibrium for the carbonaceous materials obtained.

1) Langmuir isotherm

The isotherms were plotted according to the equation (12):

2) Freundlich isotherm

This model is presented according to the relation (14):

3) Tempkin model

This model was presented according to the equation (15):

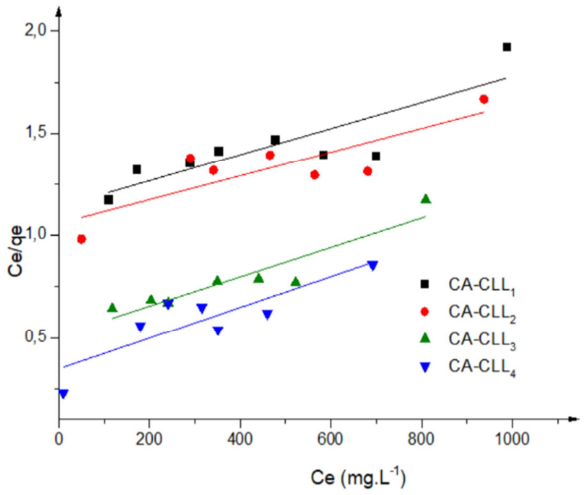

Figure 9. *Linearized forms of the Langmuir model for red Congo adsorption on activated carbons.*

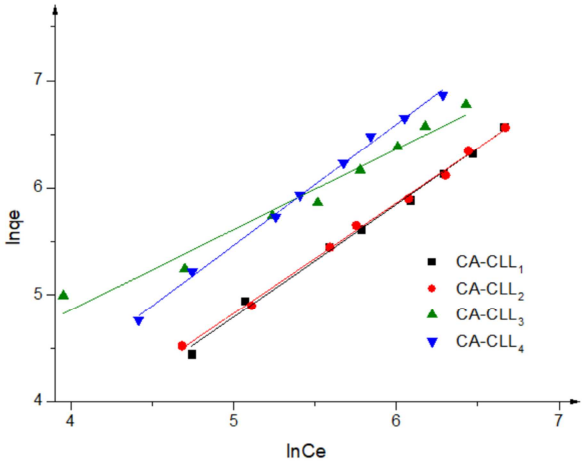

Figure 10. *Linearized forms of the Freundlich model for red Congo adsorption on activated carbons.*

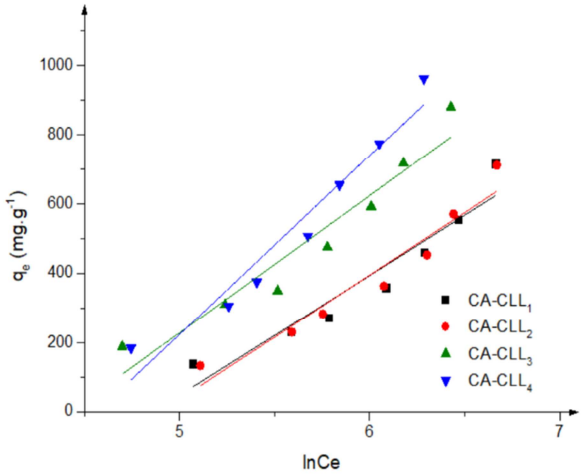

Figure 11. *Linearized forms of the Tempkin model for red Congo adsorption on activated carbons.*

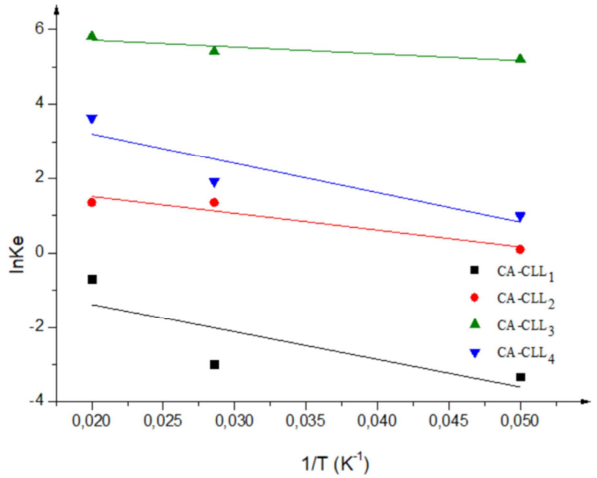

Figure 12. *Representation of the Van't Hoff equation for the adsorption of red Congo by activated carbons.*

Table 3. *Langmuir, Freundlich and Tempkin isotherms constants and their correlation coefficient for the adsorption of red Congo on activated carbons from Lophira lanceolata hulls.*

	Isotherm of Langmuir			**Isotherm of Freundlich**			**Isotherm of Tempkin**		
	q_{max} (mg/g)	**K_L (L.mg^{-1})**	**R_L^2**	**1/n**	**k_F ((mg.g^{-1}) (L.g^{-1})$^{1/n}$)**	**R_F^2**	**A (L.g^{-1})**	**B**	**R_T^2**
Congo red									
CA – CLL_1	1666,67	5,27.10-4	0,7407	1,05	0,62	0,99412	0,008	346,38	0,89588
CA – CLL_2	1587,30	5,95.10-4	0,6955	1,03	0,71	0,99672	0,007	359,05	0,92008
CA – CLL_3	1428,57	1,37.10-3	0,8728	1,10	6,39	0,96344	0,012	395,39	0,91151
CA – CLL_4	1250,00	2,30.10-3	0,7393	1,13	0,82	0,99638	0,010	515,59	0,936

Table 4. *Adsorption capacity of Congo red on different produced adsorbents.*

Precursor	**q_{max} (mg.g^{-1})**	**Reference**
Cellulose	98.14	[25]
Cellulose-GNP	139.64	[25]
CSB/ZnONPs	555.60	[26]
Litchi seeds powder	20.49	[27]
Kaolinite	547	[28]
Activated carbon from Sargassum fusiform	234	[29]

3.5. Influence of Temperature on the Adsorption of Red Congo

The results of the thermodynamic parameters obtained were shown in Table 5. From these results, it can be observed that the free energy is negative. This indicates that the adsorption of red Congo onto activated carbons is spontaneous, whatever the temperature. The free enthalpy is positive, which implies that the adsorption process is endothermic, so that the increase in temperature favors the adsorption of red Congo. The entropy variation (ΔS°) is positive, which suggests that the molecules of the two dyes fix randomly to the solid/solution interface during the adsorption process [27].

Table 5. *Thermodynamic parameters ΔG°, ΔH° and ΔS° relating to the adsorption of red Congo onto activated carbons.*

Samples	**T (K)**	**ΔG°(kJ.mol^{-1})**	**ΔH°(kJ.mol^{-1})**	**ΔS°(J.mol^{-1})**
Red Congo				
	293,15	-12,65		
CA – CLL_1	308,15	-24,84	225,72	0,81
	323,15	-37,04		
	293,15	-5503,49		
CA – CLL_2	308,15	-5804,23	373,94	20,05
	323,15	-6104,96		
	293,15	-14671,75		
CA – CLL_3	308,15	-15430,28	152,33	50,57
	323,15	-16188,80		
	293,15	-11001,44		
CA – CLL_4	308,15	-11598,04	658,11	39,77
	323,15	-12194,65		
	293,15	-616,30		
CA – CLL_4	308,15	-649,65	35,47	2,22
	323,15	-683,00		

3.6. Adsorption Mechanism of Red Congo on Activated Carbons

Figure 13 explain the mechanism of adsorption of red Congo on the surface of activated carbons. Since even if the capacity of an adsorbents to fix the molecules of a solution depends on the development of the pores, the nature of the chemical functions of the surface the latter is very important of a possible adsorption or not of the molecules [30]. Moreover, the presence on the surface of the activated carbons of acid groups such as acid and carboxylic anhydrides play two roles: (1) the reaction of carboxylic groups with red Congo to form an ester liaison; (2) the removal by these carboxylic groups of π-electrons from the aromatic [31, 32].

In sum, during adsorption, binding is due to several types of interactions, such as electrostatic interaction, hydrophobic interaction, hydrogen bonding interaction, π-π dispersion interaction and n-π interaction as shown in the figures below.

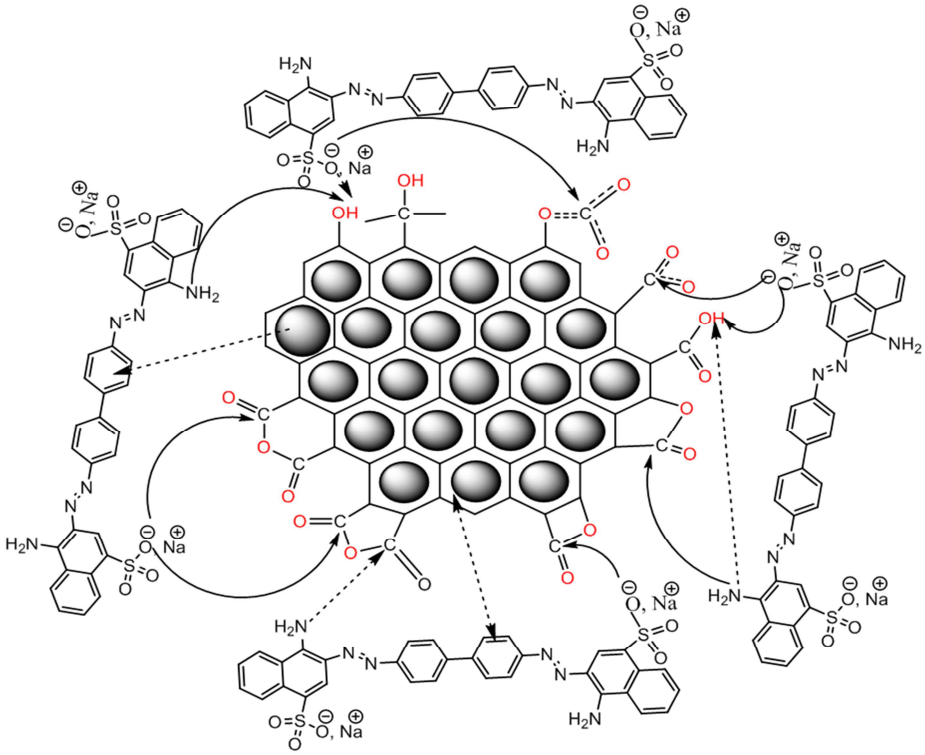

Figure 13. *Adsorption mechanisms of red Congo on activated carbons of Lophira lanceolate.*

4. Conclusion

The results obtained in this work showed that a simple pyrolysis (500°C/2 hours) preceded by an impregnation of phosphoric acid can produce activated carbons from the shells of *Lophira lanceolata* for the treatment of water contaminated with anionic pollutants. It is shown that the rate of impregnation has a great influence on the adsorption capacities of both pollutants. The adsorption of Congo red is at a removal rate of about 50%. The pseudo-second order kinetic model accurately describes the kinetics of the adsorption of the pollutants on activated carbons. The adsorption of Congo red on activated carbons is not favorable because of the anionic and complex nature of its molecules.

This study shows that the co-products generated by *Lophira lanceolata* are potential precursors of activated carbon that can be used in several fields, leading to a less polluting agriculture, a guarantee for sustainable development and a source of additional income for farmers.

Based on the results of this study, it is recommended to use activated carbons produced for low concentrations of Congo Red and they are also generally applicable to anionic dyes. It should be added that, from a methodological point of view, error functions can be used as a complement to select the most appropriate kinetic model.

Credit Author Statement

Elie SOGBOCHI: Methodology, Investigation, Formal analysis, Data curation, Validation, Writing - original project, Writing - review and editing.

Pierre GIRODS: Methodology, Investigation, Data curation, Writing - original draft, Writing - review and editing, Visualization, Validation, Formal analysis, Writing - review and editing.

Guevara NONVIHO: Methodology, Investigation, Writing - review and editing, Visualization and Supervision.

Sébastien FONTANA: Data conservation, Writing - original version, Formal analysis, and Visualization.

Yann ROGAUME.: Formal analysis, Investigation, Resources, Data retention, Supervision and Project administration.

Dominique C. K. SOHOUNHLOUE: Conceptualization, Investigation, Resources, Data retention, Supervision and Project administration.

Declaration of Competing Interest

The authors declare that they have no conflict of interests.

References

[1] B. Priyadarshini, T. Patra, and T. R. Sahoo, "An efficient and comparative adsorption of Congo red and Trypan blue dyes on MgO nanoparticles : Kinetics, thermodynamics and isotherm studies," *J. Magnes. Alloy.*, vol. 9, no. 2, pp. 478–488, 2021, doi: 10.1016/j.jma.2020.09.004.

[2] F. Li, A. R. Zimmerman, X. Hu, Z. Yu, J. Huang, and B. Gao, "One-pot synthesis and characterization of engineered hydrochar by hydrothermal carbonization of biomass with $ZnCl_2$," *Chemosphere*, vol. 254, p. 126866, 2020, doi: 10.1016/j.chemosphere.2020.126866.

[3] Z. Zhang, L. Moghaddam, I. M. O'Hara, and W. O. S. Doherty, "Congo Red adsorption by ball-milled sugarcane bagasse," *Chem. Eng. J.*, vol. 178, pp. 122–128, 2011, doi: 10.1016/j.cej.2011.10.024.

[4] A. Bazan-Wozniak, P. Nowicki, and R. Pietrzak, "Removal of NO_2 from gas stream by activated bio-carbons from physical activation of residue of supercritical extraction of hops," *Chem. Eng. Res. Des.*, vol. 166, no. 2, pp. 67–73, 2021, doi: 10.1016/j.cherd.2020.11.021.

[5] Y. Dehmani *et al.*, "Kinetic, thermodynamic and mechanism study of the adsorption of phenol on Moroccan clay," *J. Mol. Liq.*, vol. 312, 2020, doi: 10.1016/j.molliq.2020.113383.

[6] A. Dabrowski, "Adsorption ҂ from theory to practice," *Adv. Colloid Interface Sci. 93Ž.*, vol. 93, pp. 135–224, 2001.

[7] R. Zhao *et al.*, "Thermodynamic research of adsorbent materials on energy efficiency of vacuum-pressure swing adsorption cycle for CO_2 capture," *Appl. Therm. Eng.*, vol. 128, pp. 818–829, 2018, doi: 10.1016/j.applthermaleng.2017.09.074.

[8] X. Chen *et al.*, "Microporous and Mesoporous Materials Facile one-step synthesis of magnetic Zeolitic Imidazolate Framework for ultra fast removal of Congo red from water," *Microporous Mesoporous Mater.*, vol. 311, no. October 2020, p. 110712, 2021, doi: 10.1016/j.micromeso.2020.110712.

[9] A. M. Omer, E. M. Abd El-Monaem, M. M. Abd El-Latif, G. M. El-Subruiti, and A. S. Eltaweil, "Facile fabrication of novel magnetic ZIF-67 MOF@aminated chitosan composite beads for the adsorptive removal of Cr(VI) from aqueous solutions," *Carbohydr. Polym.*, vol. 265, no. April, p. 118084, 2021, doi: 10.1016/j.carbpol.2021.118084.

[10] P. González-García, "Activated carbon from lignocellulosics precursors: A review of the synthesis methods, characterization techniques and applications," *Renewable and Sustainable Energy Reviews*, vol. 82, no. August 2017. Elsevier Ltd, pp. 1393–1414, 2018. doi: 10.1016/j.rser.2017.04.117.

[11] J. Feng, K. Qiao, L. Pei, J. Lv, and S. Xie, "Using activated carbon prepared from Typha orientalis Presl to remove phenol from aqueous solutions," *Ecol. Eng.*, vol. 84, pp. 209–217, 2015, doi: 10.1016/j.ecoleng.2015.09.028.

[12] E. Sogbochi, C. K. Balogoun, C. P. A. Dossa, and D. C. K. Sohounhloue, "Evaluation of Adsorption Capacity of Methylene Blue in Aqueous Medium by Two Adsorbents: The Raw Hull of *Lophira Lanceolata* and Its Activated Carbon," *Am. J. Phys. Chem.*, vol. 6, no. 5, pp. 76–87, 2017, doi: 10.11648/j.ajpc.20170605.11.

[13] Q. Han, J. Wang, B. A. Goodman, J. Xie, and Z. Liu, "High adsorption of methylene blue by activated carbon prepared from phosphoric acid treated eucalyptus residue," *Powder Technol.*, vol. 366, pp. 239–248, 2020, doi: 10.1016/j.powtec.2020.02.013.

[14] Y. Li, J. Tang, Y. Liu, Z. Xiao, and Y. Zhang, "Concentration-driven selective adsorption of Congo red in binary dyes solution using polyacrolein : Experiments, characterization and mechanism studies," *J. Mol. Liq.*, vol. 335, p. 116230, 2021, doi: 10.1016/j.molliq.2021.116230.

[15] Z. Li *et al.*, "Adsorption of congo red and methylene blue dyes on an ashitaba waste and a walnut shell-based activated carbon from aqueous solutions: Experiments, characterization and physical interpretations," *Chem. Eng. J.*, vol. 388, no. December 2019, p. 124263, 2020, doi: 10.1016/j.cej.2020.124263.

[16] M. Kilic, E. Apaydin-Varol, and A. E. Pütün, "Adsorptive removal of phenol from aqueous solutions on activated carbon prepared from tobacco residues: Equilibrium, kinetics and thermodynamics," *J. Hazard. Mater.*, vol. 189, no. 1–2, pp. 397–403, 2011, doi: 10.1016/j.jhazmat.2011.02.051.

[17] A. M. Carvajal-bernal, F. Gómez-granados, L. Giraldo, J. Carlos, M. Balsamo, and A. Erto, "Kinetic and thermodynamic study of n-pentane adsorption on activated carbons modified by either carbonization or impregnation with ammonium hydroxide," *Microporous Mesoporous Mater.*, p. 110196, 2020, doi: 10.1016/j.micromeso.2020.110196.

[18] S. Wang and Z. H. Zhu, "Effects of acidic treatment of activated carbons on dye adsorption," *Dye. Pigment.*, vol. 75, no. 2, pp. 306–314, 2007, doi: 10.1016/j.dyepig.2006.06.005.

[19] S. Altenor, B. Carene, E. Emmanuel, J. Lambert, J. J. Ehrhardt, and S. Gaspard, "Adsorption studies of methylene blue and phenol onto vetiver roots activated carbon prepared by chemical activation," *J. Hazard. Mater.*, vol. 165, no. 1–3, pp. 1029–1039, 2009, doi: 10.1016/j.jhazmat.2008.10.133.

[20] V. Fierro, V. Torné-Fernández, D. Montané, and A. Celzard, "Adsorption of phenol onto activated carbons having different textural and surface properties," *Microporous Mesoporous Mater.*, vol. 111, no. 1–3, pp. 276–284, 2008, doi: 10.1016/j.micromeso.2007.08.002.

[21] Y. Shen, Y. Zhou, Y. Fu, and N. Zhang, "Activated carbons synthesized from unaltered and pelletized biomass wastes for bio-tar adsorption in different phases," *Renew. Energy*, vol. 146, pp. 1700–1709, 2020, doi: 10.1016/j.renene.2019.07.167.

[22] A. A. Attia, B. S. Girgis, and N. A. Fathy, "Removal of methylene blue by carbons derived from peach stones by H_3PO_4 activation: Batch and column studies," *Dye. Pigment.*, vol. 76, no. 1, pp. 282–289, 2008, doi: 10.1016/j.dyepig.2006.08.039.

[23] M. A. Al-ghouti and D. A. Da, "Guidelines for the use and interpretation of adsorption isotherm models : A review," *J. Hazard. Mater.*, vol. 393, no. February, p. 122383, 2020, doi: 10.1016/j.jhazmat.2020.122383.

[24] S. F. Lütke, A. V. Igansi, L. Pegoraro, G. L. Dotto, L. A. A. Pinto, and T. R. S. Cadaval, "Preparation of activated carbon from black wattle bark waste and its application for phenol adsorption," *J. Environ. Chem. Eng.*, vol. 7, no. 5, p. 103396, 2019, doi: 10.1016/j.jece.2019.103396.

[25] M. E. González-López, C. M. Laureano-Anzaldo, A. A. Pérez-Fonseca, C. Gómez, and J. R. Robledo-Ortíz, "Congo red adsorption with cellulose-graphene nanoplatelets beads by differential column batch reactor," *J. Environ. Chem. Eng.*, vol. 9, no. 2, 2021, doi: 10.1016/j.jece.2021.105029.

[26] M. M. Iqbal *et al.*, "Effective sequestration of Congo red dye with ZnO/cotton stalks biochar nanocomposite: MODELING, reusability and stability," *J. Saudi Chem. Soc.*, vol. 25, no. 2, p. 101176, 2021, doi: 10.1016/j.jscs.2020.101176.

[27] J. N. Edokpayi and E. Makete, "Removal of Congo red dye from aqueous media using Litchi seeds powder: Equilibrium, kinetics and thermodynamics," *Phys. Chem. Earth*, vol. 123, no. April 2020, p. 103007, 2021, doi: 10.1016/j.pce.2021.103007.

[28] S. J. Olusegun and N. D. S. Mohallem, "Comparative adsorption mechanism of doxycycline and Congo red using synthesized kaolinite supported $CoFe_2O_4$ nanoparticles*," *Environ. Pollut.*, vol. 260, p. 114019, 2020, doi: 10.1016/j.envpol.2020.114019.

[29] M. Ma, H. Ying, F. Cao, Q. Wang, and N. Ai, "Adsorption of congo red on mesoporous activated carbon prepared by CO_2 physical activation," *Chinese J. Chem. Eng.*, vol. 28, no. 4, pp. 1069–1076, 2020, doi: 10.1016/j.cjche.2020.01.016.

[30] C. K. Balogoun, I. Tchakala, M. Medokponou, M. L. Bawa, and D. C. Sohounhloue, "Influence of Pretreatment with Soda (NaOH) on the Structural Characteristics of Activated Carbon Prepared by Chemical Means with H_3PO_4 from Rice Bran," *Am. J. Phys. Chem.*, vol. 5, no. 2, pp. 35–44, 2016, doi: 10.11648/j.ajpc.20160502.13.

[31] Q. Lian, F. Islam, Z. Uddin, X. Lei, and D. Depan, "Chemosphere Enhanced adsorption of resorcinol onto phosphate functionalized graphene oxide synthesized via Arbuzov Reaction : A proposed mechanism of hydrogen bonding and π - π interactions," *Chemosphere*, vol. 280, no. January, p. 130730, 2021, doi: 10.1016/j.chemosphere.2021.130730.

[32] H. Nguyen, Y. Wang, S. You, and H. Chao, "Insights into the mechanism of cationic dye adsorption on activated charcoal : The importance of π - π interactions," *Process Saf. Environ. Prot.*, vol. 107, pp. 168–180, 2017, doi: 10.1016/j.psep.2017.02.010.